Available online at www.sciencedirect.com

SciVerse ScienceDirect

Ceramics International 39 (2013) 5765–5769

CERAMICS INTERNATIONAL

www.elsevier.com/locate/ceramint

Synthesis of nanocrystalline $LaMn_{0.5}Fe_{0.5}O_3$ powders via a PVA sol–gel route

Chunlian Zeng[a], Yanyan He[b], Changnian Li[b], Yebin Xu[b,*]

[a]School of Chemistry and Chemical Engineering, Sun Yat Sen University, Guangzhou, Guangdong 510275, China
[b]School of Optics and Electronic Information, Huazhong University of Science and Technology, Wuhan, Hubei 430074, China

Received 13 December 2012; received in revised form 28 December 2012; accepted 29 December 2012
Available online 9 January 2013

Abstract

$LaMn_{0.5}Fe_{0.5}O_3$ powders were synthesized via a sol–gel route based on polyvinyl alcohol (PVA). Differential thermal (DTA) and thermogravimetric (TG) analysis, Fourier transform infrared spectroscopy (FT-IR), X-ray diffraction (XRD) and Field emission scanning electron microscopy (FESEM) techniques were used to characterize precursors and derived oxide powders. The effect of the molar ratios of hydroxyl groups of PVA to metal ions (OH/M) on the formation of $LaMn_{0.5}Fe_{0.5}O_3$ was investigated. XRD analysis showed single-phase and well-crystallized $LaMn_{0.5}Fe_{0.5}O_3$ of around 25 nm diameters was synthesized from the OH/M = 1.5 precursor at 600 °C. For the precursor with OH/M = 0.75, phase pure $LaMn_{0.5}Fe_{0.5}O_3$ was not obtained even at 1000 °C and $La(OH)_3$ was observed as impurity phase. $LaMn_{0.5}Fe_{0.5}O_3$ ceramics sintered at 1300 °C showed a dielectric constant of 4300 at room temperature and 100 kHz.

Keywords: A. Powders: chemical preparation; A. Sol–gel process; D. Perovskites

1. Introduction

Perovskite oxides ABO_3 are an important class of materials, characterized by subtle structural distortions from the cubic aristotype structure. They have very important structural, electrical and magnetic properties. These important materials have received a large amount of academic interest and can be used as oxygen-permeation membranes, partial-oxidation catalysts or components of a solid-oxide fuel cell [1–3]. Recently, it is reported that some double perovskite structure oxides $A_2BB'O_6$ (A-rare earth, B and B'-3d transition metals) exhibited colossal magnetodielectric behavior [4,5], giant dielectric constant [6–8] and giant dielectric tunability [8–10]. Among the rare earth-based double perovskite oxides, $LaMn_{1-x}Fe_xO_3$ was widely studied for its dielectric, magnetic, transport and catalytic properties [3,6,8,11–13]. Generally, $LaMn_{1-x}Fe_xO_3$ was prepared by solid-state reactions at high temperatures [14,15]. This technique has several problems, e.g., poor homogeneity and high porosity of the samples, no control on the particle size, etc. To overcome these drawbacks, several wet chemical methods including sol–gel method [3,6,12], glycine nitrate method [11,13] and citrate autocombustion method [16] have been proposed.

PVA solution polymerization method has been used successfully to synthesize various monophases, fine, and pure mixed-oxide powders [17–21], but no literature currently reports the synthesis of $LaMn_{0.5}Fe_{0.5}O_3$. In the present paper, the sol–gel method based on PVA was used to prepare nanocrystalline $LaMn_{0.5}Fe_{0.5}O_3$ powders and the effect of PVA content on the formation of $LaMn_{0.5}Fe_{0.5}O_3$ was investigated. Single phase $LaMn_{0.5}Fe_{0.5}O_3$ has been successfully prepared at lower temperature.

2. Experimental procedure

$LaMn_{0.5}Fe_{0.5}O_3$ nanoparticles were prepared by the PVA based sol–gel method. The method has been described previously [20,21]. In this method, high purity La_2O_3, $MnCO_3$ and $Fe(NO_3)_2 \cdot 9H_2O$ were taken as the raw materials. First, a 5 wt% PVA (MW = 79,000) solution was made by adding PVA to deionized water. The polymer

*Corresponding author. Tel.: +86 27 87553855; fax: +86 27 87543427.
E-mail addresses: xuyebin@yahoo.com, xu-ye-bin@163.com (Y. Xu).

0272-8842/$ - see front matter © 2013 Elsevier Ltd and Techna Group S.r.l. All rights reserved.
http://dx.doi.org/10.1016/j.ceramint.2012.12.094

was dissolved by stirring at a temperature of about 80 °C. La_2O_3 and $MnCO_3$ were dissolved in nitric acid and mixed with PVA solution with stirring. Then stoichiometric $Fe(NO_3)_3 \cdot 9H_2O$ was added. During the process, the molar ratios of hydroxyl groups of PVA to metal ions (OH/M) were 0.75, and 1.5, respectively. The solution was continuously stirred and kept at a temperature of 80 °C until a sticky gel was formed. Subsequently, the sample breaker was removed from the hot plate and heated in an oven at 250 °C for 2 h. The resulting mass was slightly ground into a fine powder and the $LaMn_{0.5}Fe_{0.5}O_3$ precursor was obtained. Finally, the powder precursor was calcined at 500–1000 °C in air for 2 h to obtain $LaMn_{0.5}Fe_{0.5}O_3$ powders. The powders heated at 800 °C for 2 h were pressed into disks 12 mm in diameter and 1–2 mm thickness at a pressure of 100 MPa. The disks were sintered in air at 1300 °C for 3 h.

Simultaneous differential thermal (DTA) and thermogravimetric (TG) analysis (Diamond TG/DTA, Perkin Elmer Instruments) at a heating rate of 10 °C min^{-1} in static air were used to monitor the decomposition and pyrolysis of the precursor. Fourier transform infrared spectroscopy (FT-IR, Vertex 70, Bruker) was used to determine the chemical bonding of the $LaMn_{0.5}Fe_{0.5}O_3$ powders. The phases of the samples were determined by powder X-ray diffraction (XRD) using Cu Kα radiation (X'Pert PRO, PANalytical B.V.). The grain size and morphology of $LaMn_{0.5}Fe_{0.5}O_3$ powders were examined by Hitachi S-4800 field emission scanning electron microscopy (Hitachi Ltd., Tokyo, Japan).

The disk samples were polished to produce flat uniform surfaces and electroded with lead-free silver paint (Wuhan Youle Optoelectronic Technology Co. Ltd., SA-5121, Wuhan, China). The painted samples were heated at 600 °C for 8 min. The dielectric constant and loss tangent of the samples were measured using Triton DS6000 Dielectric Thermal Analyzer at 100 kHz in the temperature range from 20 °C to 100 °C with a heating rate of 5 °C/min.

3. Results and discussion

Fig. 1 shows the results of DTA and TG analysis for the $LaMn_{0.5}Fe_{0.5}O_3$ precursor with OH/M = 1.5. The precursor exhibits three distinct stages of decomposition in TG curve. The first weight loss shown by TG curve is indicative of the dehydration of the precursor. The second large weight loss between 200 °C and 580 °C can be ascribed to the decomposition of most of the organics by oxidation and the release of N_xO_y, CO, and CO_2 gases. The last weight loss between 580 °C and 690 °C is associated with the oxidation of residual organics. No more weight loss was observed in the temperature range from 690 °C to 950 °C. In the DTA curve, no clear endothermal or exothermal peak was observed. Therefore, there is no evidence of a phase transition taking place in the sample up to a temperature of 950 °C.

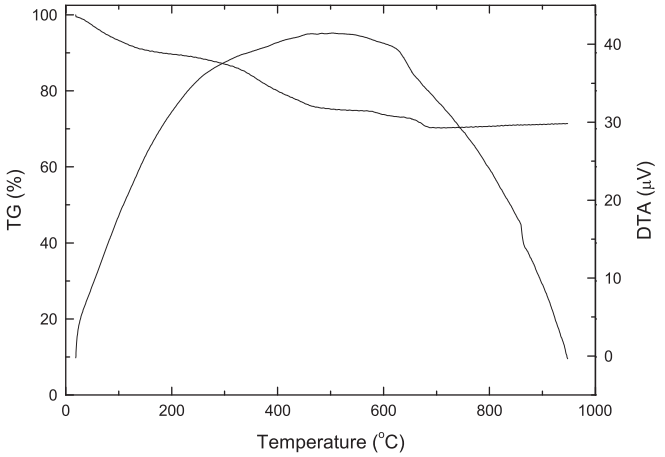

Fig. 1. DTC/TG curves of $LaMn_{0.5}Fe_{0.5}O_3$ precursor with OH/M = 1.5.

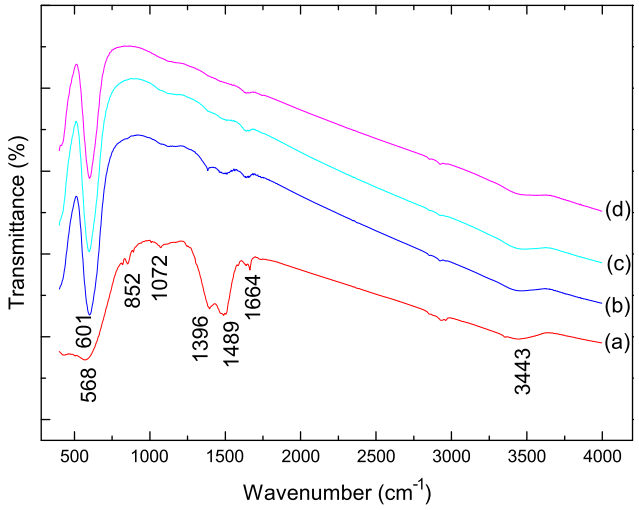

Fig. 2. FT-IR spectra of $LaMn_{0.5}Fe_{0.5}O_3$ precursor (OH/M = 1.5) calcined at 500–900 °C. (a) 500 °C, (b) 600 °C, (c) 800 °C and (d) 900 °C.

Fig. 2 shows the FT-IR spectra obtained from the $LaMn_{0.5}Fe_{0.5}O_3$ precursor (OH/M = 1.5) calcined at various temperatures in the wavenumber range from 400 to 4000 cm^{-1}. For the precursor calcined at 400 °C, the absorption band at about 1489 and 1396 cm^{-1} can be assigned to the splitting of the ν_3 asymmetric stretching of metal carbonates [22] while the other bands at about 1072 and 852 cm^{-1} are attributed to the ν_1 and ν_2 modes of the carbonate ions, respectively [23]. The broad absorption band in the range of 3437 cm^{-1} is due to O–H stretching. In addition, the bands at about 1664 cm^{-1} can be ascribed to the asymmetric COO^- stretching vibrations. There is no COO^- in PVA units; however, some hydroxyl groups of PVA units can be oxidized to COO^- by the excess HNO_3. At a calcination temperature of 600 °C, the intensities of bands related to carbonate decrease greatly, and a well-established strong absorption band at 601 cm^{-1} indicates the formation of $LaMn_{0.5}Fe_{0.5}O_3$. For the perovskite ABO_3, the B–O bond stretching vibration of the BO_6 octahedra (ν_1 of the IR active F1u mode of vibration) is

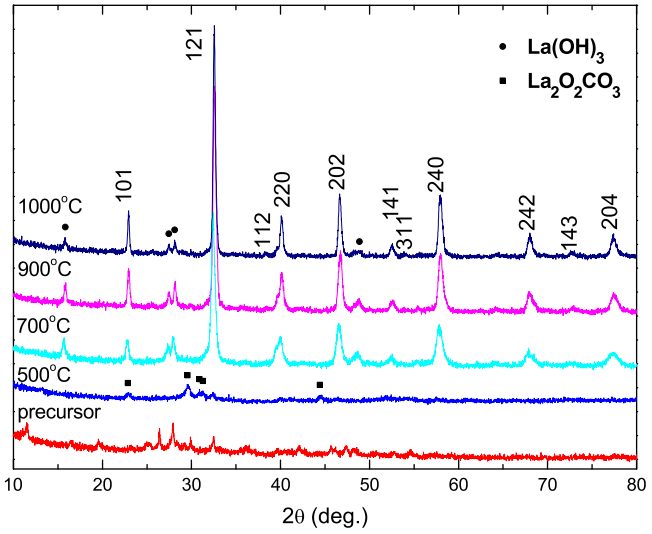

Fig. 3. XRD patterns of the $LaMn_{0.5}Fe_{0.5}O_3$ precursor (OH/M=0.75) calcined at various temperatures for 2 h.

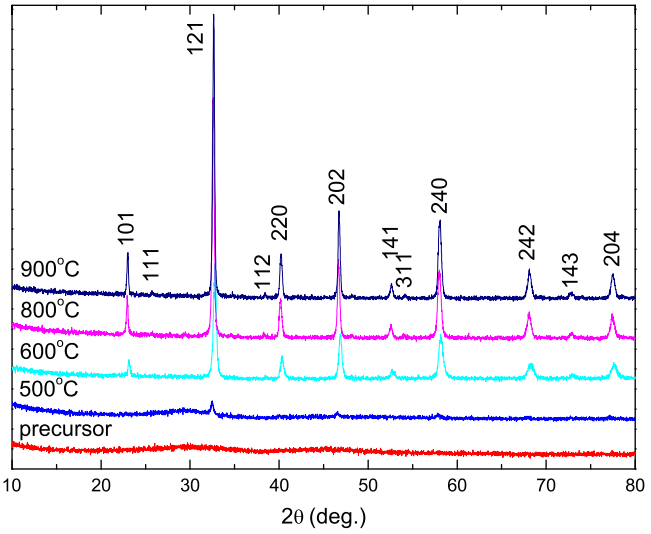

Fig. 4. XRD patterns of the $LaMn_{0.5}Fe_{0.5}O_3$ precursor (OH/M=1.5) calcined at various temperatures for 2 h.

observed in the 500–700 cm^{-1} region [11,24,25]. The 601 cm^{-1} band is due to the joint action of the Mn–O and Fe–O stretching vibrations. This is consistent with Ref. [24] where this band was observed at 606 cm^{-1}. Increasing calcination temperature to 800 and 900 °C further, the spectra show no obvious change.

The XRD patterns of the $LaMn_{0.5}Fe_{0.5}O_3$ precursor (OH/M=0.75) calcined at various temperatures for 2 h are shown in Fig. 3. In the precursor, only the reflections from $La(OH)_2NO_3$ (ICCD file 26-1146) are observed. Heating the precursor at 500 °C for 2 h, $LaMn_{0.5}Fe_{0.5}O_3$ phase starts to crystallize, but $La_2O_2CO_3$ is the major phase. At 700 °C, $La_2O_2CO_3$ phase disappears and a mixture of $LaMn_{0.5}Fe_{0.5}O_3$ and $La(OH)_3$ is obtained, with $LaMn_{0.5}Fe_{0.5}O_3$ as the major phase. Increasing calcination temperature to 900 °C and 1000 °C, the reflections from $La(OH)_3$ can still be observed. Therefore, phase pure $LaMn_{0.5}Fe_{0.5}O_3$ cannot be obtained from the precursor with OH/M=0.75, even at a temperature as high as 1000 °C.

Fig. 4 shows the XRD patterns of the $LaMn_{0.5}Fe_{0.5}O_3$ precursor (OH/M=1.5) calcined at various temperatures for 2 h. The precursor is primarily amorphous in structure. Calcining precursor at 500 °C for 2 h, some weak reflections from $LaMn_{0.5}Fe_{0.5}O_3$ appear, but the continuum around $2\theta=29.2°$ indicates the existence of amorphous substance. This is consistent with the FT-IR results. Increasing calcination temperature to 600 °C, all the reflections in the XRD patterns correspond to a perovskite structure, indicating the formation of single phase compound $LaMn_{0.5}Fe_{0.5}O_3$. The reflections could be indexed on a $GdFeO_3$ type orthorhombic perovskite lattice with the space group Pbnm [12,13]. With increasing heating to 800 °C and 900 °C, the diffraction peaks become stronger and sharper, reflecting greater crystallization. No other significant changes are observed. The lattice parameters were calculated using a least-squares refinement program [26] and the result is as follow: $a=0.554458$ nm, $b=0.780790$ nm and $c=0.552158$ nm. These values are comparable to the values reported [13]. The average crystallite sizes of the synthesized powders are also determined according to the X-ray line-broadening of the (121) diffraction peak using Scherrer's equation: $D=0.89\lambda/B\cos\theta$, where D is the crystallite size; λ is the X-ray wavelength (0.15406 nm for Cu K_α); B is the corrected FWHM of the diffraction peak; and θ corresponds to the diffraction angle. The average crystallite size was about 38.3 nm for the powders calcined at 800 °C. Therefore, we can see that increasing PVA content resulted in the formation of single-phase $LaMn_{0.5}Fe_{0.5}O_3$ at 600 °C.

Fig. 5 shows the field emission scanning electron microscopy micrographs of $LaMn_{0.5}Fe_{0.5}O_3$ precursor with CA/M=2 calcined at 600 °C and 800 °C for 2 h. $LaMn_{0.5}Fe_{0.5}O_3$ nanoparticles with a diameter of about 25 nm were obtained at 600 °C. As expected, the sample that have been calcined at 800 °C shows bigger particle size (~40 nm) which is consistent with that calculated from the XRD peak widths by Scherrer's equation.

The main function of PVA is to provide a polymeric network to hinder cation mobility allowing local stoichiometry to be maintained and minimizing precipitation of unwanted phases. On the other hand, PVA can also act as fuel during calcination. Increasing PVA content results in more OH groups. On one hand, the uniformity of metal element in the solution and precursor was improved; on the other hand, the potential heat of combustion produced during calcination was increased. Hence, increasing the PVA content enhances the formation of $LaMn_{0.5}Fe_{0.5}O_3$. Similar results can also be found in the synthesis of $LaFeO_3$ via the PVA sol–gel method [21]. For the precursor with OH/M=1.5, $LaFeO_3$ was formed directly in the charring procedure, but phase pure $LaFeO_3$ was obtained from the precursor with OH/M=0.75 at 700 °C.

Fig.6 shows the variation of dielectric constant as a function of temperature at a frequency of 100 kHz. The variation of loss tangent ($\tan\delta$) is also plotted in this

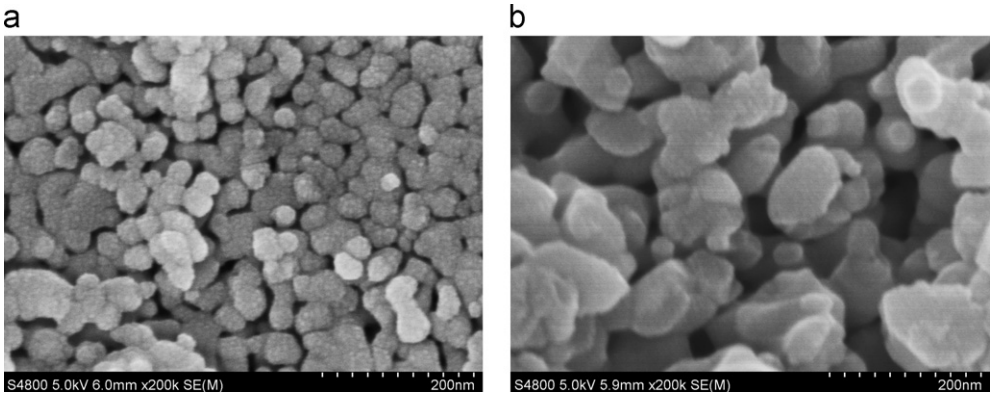

Fig. 5. FESEM micrographs of $LaMn_{0.5}Fe_{0.5}O_3$ precursor (OH/M = 1.5) calcined at (a) 600 °C and (b) 800 °C for 2 h.

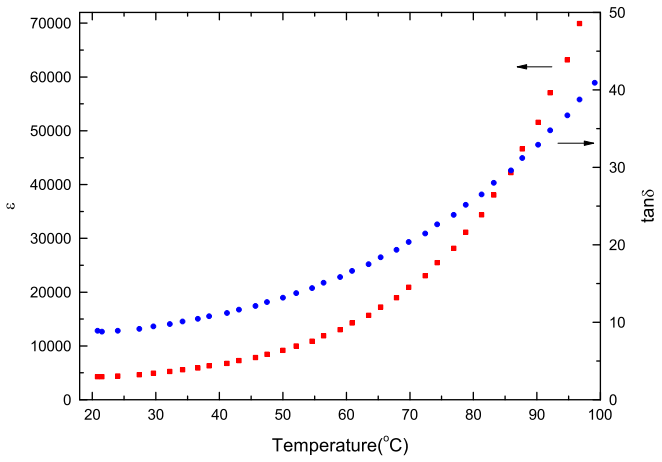

Fig. 6. Variation of dielectric constant (ε) and loss tangent ($\tan\delta$) of the $LaMn_{0.5}Fe_{0.5}O_3$ ceramics as a function of temperature at 100 kHz frequency.

figure. The dielectric constant around room temperature is 4300, which is smaller than that Karmakar et al. [6] and Dong et al. [8] reported. The loss tangent around room temperature is about 9. This value is comparable to that in $LaMn_{0.5}Co_{0.5}O_3$ [27] and La_2NiMnO_6 systems [9]. In Ref. [6,8], no loss tangent was provided. The dielectric constant and loss tangent increase monotonically with the increase of temperature. We measured the dielectric constant of the sample under an applied electric field using Agilent 4294A precision impedance analyzer, no dielectric tunability as in the La_2NiMnO_6 system [9] was observed.

4. Conclusion

The PVA based sol–gel method has been used to synthesize $LaMn_{0.5}Fe_{0.5}O_3$. The effects of the molar ratios of hydroxyl groups of PVA to metal ions (OH/M) on the formation of $LaMn_{0.5}Fe_{0.5}O_3$ were studied. For the precursor with OH/M = 0.75, phase pure $LaMn_{0.5}Fe_{0.5}O_3$ was not synthesized even at 1000 °C, and $La(OH)_3$ phase was observed as impurity. Increasing PVA content to OH/M = 1.5, single-phase and well-crystallized $LaMn_{0.5}Fe_{0.5}O_3$ powders of around 25 nm diameter was synthesized at 600 °C. $LaMn_{0.5}Fe_{0.5}O_3$ ceramics sintered at 1300 °C had a dielectric constant of 4300 at room temperature and 100 kHz.

Acknowledgments

This work is supported by the Natural Science Foundation of China under Grant nos. 10975055 and 60771021. The authors wish to acknowledge the Analytical and Testing Center in Huazhong University of Science and Technology for XRD and FT-IR analysis.

References

[1] J.B. Goodenough, Electronic and ionic transport properties and other physical aspects of perovskites, Reports on Progress in Physics 67 (2004) 1915–1993.
[2] T. Komatsu, H. Arai, R. Chiba, K. Nozawa, M. Arakawa, K. Sato, Long-term chemical stability of $LaNi(Fe)O_3$ as a cathode material in solid oxide fuel cells, Journal of the Electrochemical Society 154 (2007) B379–B382.
[3] M.J. Koponen, T. Venalainen, M. Suvanto, K. Kallinen, T.J. Kinnunen, M. Harkonen, T.A. Pakkanen, Methane conversion and SO_2 resistance of $LaMn_{1-x}Fe_xO_3$ (x=0.4, 0.5, 0.6 and 1) perovskite catalysts promoted with palladium, Journal of Molecular Catalysis A: Chemical 258 (2006) 246–250.
[4] N.S. Rogado, J. Li, A.W. Sleight, M.A. Subramanian, Magnetocapacitance and magnetoresistance near room temperature in a ferromagnetic semiconductor: La_2NiMnO_6, Advanced Materials 17 (2005) 2225–2227.
[5] D. Choudhury, P. Mandal, R. Mathieu, A. Hazarika, S. Rajan, A. Sundaresan, U.V. Waghmare, R. Knut, O. Karis, P. Nordblad, D.D. Sarma, Near-room-temperature colossal magnetodielectricity and multiglass properties in partially disordered La_2NiMnO_6, Physical Review Letters 108 (2012) 127201.
[6] A. Karmakar, S. Majumdar, A.K. Singh, S. Giri, Intragrain electrical inhomogenities and compositional variation of static dielectric constant in $LaMn_{1-x}Fe_xO_3$, Journal of Physics D: Applied Physics 42 (2009) 092004.
[7] K.D. Chandrasekhar, A.K. Das, A. Venimadhav, Spin glass behaviour and extrinsic origin of magnetodielectric effect in non-multiferroic La2NiMnO6 nanoparticles, Journal of Physics: Condensed Matter 24 (2012) 376003.
[8] S. Dong, Y. Hou, Y. Yao, Y. Yin, D. Ding, Q. Yu, X. Li, Magnetodielectric effect and tunable dielectric properties of $LaMn_{1-x}Fe_xO_3$, Journal of the American Ceramic Society 93 (2010) 3814–3818.
[9] M.H. Tang, J.W. Hou, J. Zhang, G.J. Dong, W. Shu, The giant dielectric tunability effect in bulk La_2NiMnO_6 around room temperature, Solid State Communications 150 (2010) 1453–1456.

[10] M.H. Tang, Y.G. Xiao, B. Jiang, J.W. Hou, J.C. Li, J. He, The giant dielectric tunability effect in bulk Y_2NiMnO_6 around room temperature, Applied Physics A 105 (2011) 679–683.
[11] S.D. Bhame, V.L.J. Joly, P.A. Joy, Effect of disorder on the magnetic properties of $LaMn_{0.5}Fe_{0.5}O_3$, Physical Review B 72 (2005) 054426.
[12] K. De, R. Ray, R.N. Panda, S. Giri, H. Nakamura, T. Kohara, The Effect of Fe substitution on magnetic and transport properties of $LaMnO_3$, Journal of Magnetism and Magnetic Materials 288 (2005) 339–346.
[13] X.D. Zhou, L.R. Pederson, Q. Cai, J. Yang, B.J. Scarfino, M. Kim, W.B. Yelon, W.J. James, H.U. Anderson, C. Wang, Structural and magnetic properties of $LaMn_{1-x}Fe_xO3$ $(0 < x < 1.0)$, Journal of Applied Physics 99 (2006) 08M918.
[14] M.A. Gilleo, Crystallographic studies of perovskite-like compounds. III. La(Mx, Mn_{1-x})O_3 with M = Co, Fe and Cr, Acta Crystallographica 10 (1957) 161–166.
[15] D.V. Karpinsky, I.O. Troyanchuk, V.V. Sikolenko, Inhomogeneous magnetic states in Fe and Cr substituted $LaMnO_3$, Journal of Physics: Condensed Matter 19 (2007) 036220.
[16] P.P. Hankare, M.R. Kadam, P.D. Kamble, S.D. Jadhav, U.B. Sankpal, R.P. Patil, V.B. Helavi, N.S. Gajbhiye, Synthesis, characterization and electrical properties of the system $LaMn_x$-$Fe_{1-x}O_3$, Journal of Alloys and Compounds 489 (2010) 233–236.
[17] S.K. Saha, S. Pathak, P. Pramanik, Low-temperature preparation of fine particles of mixed oxide systems, Journal of Materials Science Letters 14 (1995) 35–37.
[18] M.A. Gulgun, M.H. Nguyen, W.M. Kriven, Polymerized organic-inorganic synthesis of mixed oxides, Journal of the American Ceramic Society 82 (1999) 556–560.
[19] M.H. Nguyen, S. Lee, W.M. Kriven, Synthesis of oxide powders by way of a polymeric steric entrapment precursor route, Journal of Materials Research 14 (1999) 3417–3426.
[20] T. Liu, Y.B. Xu, J.Y. Zhao, Low temperature synthesis of $BiFeO_3$ via the PVA sol–gel route, Journal of the American Ceramic Society 93 (2010) 3637–3641.
[21] J.S. Feng, T. Liu, Y.B. Xu, J.Y. Zhao, Y.Y. He, Effects of PVA content on the synthesis of $LaFeO_3$ via the sol–gel route, Ceramics International 37 (2011) 1203–1207.
[22] G. Busca, V. Lorenzelli, Infrared spectroscopic identification of species arising from reactive adsorption of carbon oxides on metal oxide surfaces, Materials Chemistry 7 (1982) 89–126.
[23] A.A. Davydov, Infrared Spectroscopy of Adsorbed Species on the Surface of Transition Metal Oxides, Wiley, New York, 1990.
[24] Y. Wu, Z. Yu, S. Liu, Preparation, crystal structure, and vibrational spectra of perovskite-type mixed oxides $LaM_yM_{1-y'}O_3$ (M, M′ = Mn, Fe, Co), Journal of Solid State Chemistry 112 (1994) 157–160.
[25] G.V.S. Rao, C.N.R. Rao, J.R. Ferraro, Infrared and electronic spectra of rare earth perovskites: ortho-chromites, -manganites and -ferrites, Applied Spectroscopy 24 (1970) 436–445.
[26] T.J.B. Holland, S.A.T. Redfern, Unit cell refinement from powder diffraction data: the use of regression diagnostics, Mineralogical Magazine 61 (1997) 65–77.
[27] S. Yanez-Vilar, A. Castro-Couceiro, B. Rivas-Murias, A. Fondado, J. Mira, J. Rivas, M.A. Senarıs-Rodrıgueza, Study of the dielectric properties of the perovskite $LaMn_{0.5}Co_{0.5}O_{3-\delta}$, Zeitschrift fur Anorganische und Allgemeine Chemie 631 (2005) 2265–2272.